# Interface Dzyaloshinskii-Moriya interaction in the interlayer antiferromagnetic-exchange coupled Pt/CoFeB/Ru/CoFeB systems

M. Belmeguenai,[1,*] H. Bouloussa,[1] Y. Roussigné,[1] M. S. Gabor,[2] T. Petrisor, Jr.,[2] C. Tiusan,[2,3] H. Yang,[4] A. Stashkevich,[1] and S. M. Chérif[1]

[1]*LSPM, CNRS-Université Paris 13, 99 Avenue Jean-Baptiste Clément, F-93430 Villetaneuse, France*

[2]*Center for Superconductivity, Spintronics and Surface Science, Physics and Chemistry Department, Technical University of Cluj-Napoca, Strada Memorandumului No. 28, RO-400114 Cluj-Napoca, Romania*

[3]*Institut Jean Lamour, CNRS, Université de Lorraine, F-54506 Vandoeuvre, France*

[4]*Department of Electrical and Computer Engineering, National University of Singapore, Singapore 117576, Singapore*

(Received 22 June 2017; published 2 October 2017)

Interface Dzyaloshinskii-Moriya interactions (iDMIs) in interlayer exchange coupled (IEC) Pt/$Co_{20}Fe_{60}B_{20}$(1.12 nm)/Ru/$Co_{20}Fe_{60}B_{20}$(1.12 nm) systems have been studied theoretically and experimentally. A vibrating sample magnetometer has been used to measure their magnetization at saturation and their interlayer exchange coupling constants. The latter are found to be of an antiferromagnetic nature for the investigated Ru range thickness (0.5–1 nm). Their dynamic magnetic properties were studied using the Brillouin light scattering (BLS) technique. The BLS measurements reveal pronounced nonreciprocal spin-wave propagation. In contrast to the calculations for symmetrical IEC CoFeB layers, this experimental nonreciprocity is Ru thickness and thus coupling strength dependent. Therefore, to explain the experimental behavior, a theoretical model based on the perpendicular interface anisotropy difference between the bottom and top CoFeB layers has been developed. We show that the Ru thickness dependence of the spin-wave nonreciprocity is well reproduced by considering a constant iDMI and different perpendicular interfacial anisotropy fields between the top and bottom CoFeB layers. This anisotropy difference has been confirmed by the investigation of the CoFeB thickness dependence of the effective magnetization of Pt/CoFeB/Ru and Ru/CoFeB/MgO individual layers, where a linear behavior has been observed.

DOI: 10.1103/PhysRevB.96.144402

## I. INTRODUCTION

The exchange interaction plays an important role in magnetism and therefore is responsible for several phenomena in magnetic materials. This interaction can be direct (involving an overlap of electron wave functions from the neighboring atoms and the Coulomb electrostatic interaction) or indirect (little or no direct overlap between the neighboring electrons and mediated through intermediary atoms). A direct exchange interaction between electrons arises from the Coulomb interaction and is responsible for microscopic magnetic behavior. It may contain symmetric and asymmetric terms. The symmetric term, commonly known as the Heisenberg [1] interaction, usually leads to collinear magnetic structures. The asymmetric exchange, referred to as the Dzyaloshinskii-Moriya interaction [2,3] (DMI), favors canted neighboring spins leading to various magnetization structures at the nanoscale, such as helices [4] and skyrmions [5–7]. It changes the static and dynamic properties of domain walls [8] and leads to different energies (nonreciprocity) of two spin waves (SWs) having the same wavelength and propagating along two opposite directions [9]. It is manifested by a difference between the frequencies of these two SWs. The DMI constant determination is thus reduced to this simple frequency difference measurement. Several experimental methods [10–12], largely based on how this interaction alters the properties of domain walls, were employed recently, but Brillouin light scattering (BLS) spectroscopy remains the most direct method for DMI characterization. This scheme is simple, efficient, reliable, and straightforward since few parameters are required for the experimental data fit [13,14]. It also allows for the investigation of both in-plane and perpendicular spontaneously magnetized films, in contrast to domain wall techniques. DMI can be induced by a lack of inversion symmetry of the compound and a strong spin-orbit coupling. This can be achieved by using heavy metal/ferromagnet (HM/FM) heterostructures, giving rise to interface DMIs.

Indirect exchange interactions, such as coupling between two magnetic layers separated by a nonmagnetic spacer layer, are mediated by conduction electrons of the spacer layer which are scattered successively by the magnetic layers. The coupling, which oscillates in sign as function of the thickness of the spacer layer [15,16] was first observed by Grünberg [17] for transition metal systems. It is crucial for many applications in modern magnetic storage devices and spin electronics [18]. In practice, antiferromagnetic interlayer coupling is easily revealed and measured by performing a magnetization measurement as function of the applied magnetic field. Ferromagnetic coupling is much more difficult to detect and to measure quantitatively by these static techniques, since the application of an external magnetic field has no direct action on the mutual orientations of the magnetizations of the successive magnetic layers. Therefore, dynamic methods such as ferromagnetic resonance and Brillouin light scattering remain the most powerful and used means for the precise characterization of both coupling types. Indeed, in these methods and in analogy with coupled harmonic oscillators, the magnon modes in two magnetic films coupled via a nonmagnetic interlayer can be classified into acoustic and optic

*belmeguenai.mohamed@univ-paris13.fr

 

modes depending on whether the two film magnetizations precess in phase or out of phase, respectively [19]. The behavior of the spin-wave frequencies as function of applied fields provides a great deal of information about the magnitude and functional form of the coupling energy.

Recently, Chen *et al.* [20] demonstrated an experimental approach to stabilize a room-temperature skyrmion ground state in chiral magnetic films via interlayer exchange coupling (IEC). Indeed, Shawn *et al.* [21] have reported on the direct imaging of chiral spin structures including skyrmions in an exchange coupled thick ferromagnetic Co/Pt multilayer at room temperature with Lorentz transmission electron microscopy. Moreover, it is of utmost importance to investigate the spin-wave spectrum in the presence of both DMI and IEC. Therefore, both experimental and theoretical investigations of this aspect will be reported in this paper. We thus use BLS combined with vibrating sample magnetometry (VSM) to measure the combined effects of the IEC strength and of the DMI constant on SW nonreciprocity in $Pt/Co_{20}Fe_{60}B_{20}/Ru/Co_{20}Fe_{60}B_{20}$. We show that although the two ferromagnetic (FM) layers are similar with the same thickness, caution should be paid to the interpretation of the SW nonreciprocity. Indeed, the frequency difference between the two counterpropagating SWs, usually attributed to DMI, is also IEC strength dependent when the two FM layers present different perpendicular surface anisotropies.

## II. SAMPLES AND EXPERIMENTAL TECHNIQUES

A series of $Co_{20}Fe_{60}B_{20}$(1.12 nm)/Ru($t_{Ru}$)/$Co_{20}Fe_{60}B_{20}$(1.12 nm) multilayers ($t_{Ru} = 0.5, 0.6, 0.8$, and 1 nm) have been grown by a sputtering magnetron system at room temperature on a thermally oxidized Si substrate. Prior to the deposition of the multilayer, a Ta(3 nm)/Pt(3 nm) buffer bilayer was deposited on the substrates. Finally, the trilayer was coated by a bilayer of MgO(1 nm)/Ta(3 nm). In this system, the Pt bottom layer induces perpendicular magnetic anisotropy and DMI whereas the Ru spacer layer is thought to only induce perpendicular anisotropy and to ensure IEC. The Ru thickness had been chosen in order to induce antiferromagnetic IEC between CoFeB layers. In order to determine the interface perpendicular anisotropy and the DMI constants, the individual layers Ta(3 nm)/Pt(3 nm)/Ru(0.8 nm)/CoFeB($t_{CFB}$)/MgO(1 nm)/Ta(3 nm) and Ta(3 nm)/Pt(3 nm)/CoFeB($t_{CFB}$)/Ru(0.8 nm)/Ta(3 nm) of variable CoFeB thicknesses ($0.9\text{nm} \leqslant t_{CFB} \leqslant 5\,\text{nm}$) have also been grown in the same conditions.

VSM has been used to measure the hysteresis loops of the samples with the field applied parallel to the sample plane and to obtain the intrinsic value of the magnetization at saturation ($M_s$). The BLS technique gives access to SW modes as well as phonons with nonzero wave-vector values. In the BLS setup, the SW, of a wave number ($k_{SW}$) in the range 0–20 rad/$\mu$m [depending on the incidence angle $\theta_{inc}$, $k_{SW} = \frac{4\pi}{\lambda}\sin(\theta_{inc})$ in a backscattering configuration], are probed by illuminating the sample with a laser having a wavelength $\lambda = 532\,\text{nm}$. The spectrometer is a JR Sandercock product based on a tandem Fabry-Perot interferometer. In order to select the SW lines, a crossed polarizer is placed on the path of the backscattered light from the sample. The magnetic field is applied perpendicular to the incidence plane, which allows one to probe SWs

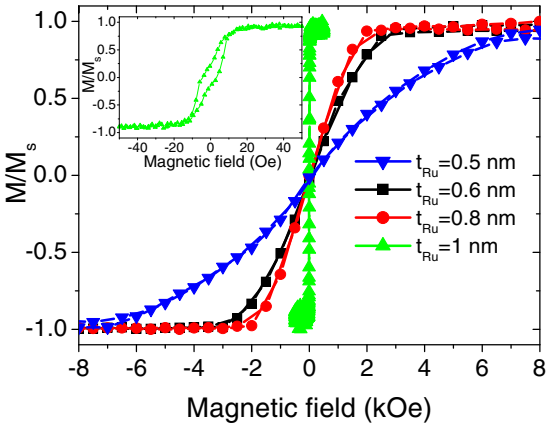


FIG. 1. VSM hysteresis loops showing the normalized in-plane magnetization component as function of the in-plane applied magnetic field for Pt/CoFeB(1.12 nm)/Ru($t_{Ru}$)/CoFeB(1.12 nm)/MgO systems of various Ru thicknesses ($t_{Ru}$). The inset shows a zoom on the hysteresis loop for $t_{Ru} = 1$ nm.

propagating along the in-plane direction perpendicular to the applied field, i.e., the Damon-Eshbach (DE) geometry, where the interface Dzyaloshinskii-Moriya interaction (iDMI) effect on the SW propagation nonreciprocity is maximal [22]. For each angle of incidence, the spectra will be obtained after sufficiently counting photons to have well-defined spectra where the line position can be determined with an accuracy of better than 0.2 GHz. The Stokes (S, negative frequency shift relative to the incident light as a magnon was created) and anti-Stokes (AS, positive frequency shift relative to the incident light as a magnon was absorbed) frequencies, detected simultaneously, will then be determined from Lorentzian fits to the BLS spectra. All the measurements presented here were carried out at room temperature.

## III. RESULTS AND DISCUSSIONS

VSM hysteresis loops for a CoFeB/Ru/CoFeB trilayer with different Ru layer thicknesses are shown in Fig. 1. These loops clearly show that for all the samples, the magnetizations of the two CoFeB layers are antiferromagnetically coupled. Indeed, in zero applied magnetic fields, the magnetizations of successive magnetic layers are antiparallel to each other, resulting in zero remnant magnetization due to the antiferromagnetic interaction. When an external magnetic field is applied, the Zeeman energy tends to align the magnetizations of both layers in the field direction, so that the magnetizations progressively increase until a saturation field is reached. This saturation field is Ru thickness dependent, as shown in Fig. 1. The in-plane saturation field allows one to derive the antiferromagnetic coupling constants. Since the variation of the magnetization versus the applied field before saturation is linear (Fig. 1), only the bilinear coupling constant $J_1$ has to be considered. Assuming in-plane magnetizations, one writes the energy per unit area as

$$E = -t_{CFB} H M_s \cos(\varphi_{M1} - \varphi_H) - t_{CFB} H M_s \cos(\varphi_{M2} - \varphi_H) - J_1 \cos(\varphi_{M1} - \varphi_{M2}). \quad (1)$$

In the above expression, the in-plane anisotropy has been neglected, and $\varphi_{M1}$, $\varphi_{M2}$, and $\varphi_H$, respectively, represent the

in-plane (referring to the substrate edge) angles defining the direction of the magnetization of the two CoFeB layers and of the applied magnetic field. The energy $E$ is minimal for $\varphi_{M1} = \varphi_{M2} = \varphi_H$ if $H > -2J_1/(t_{CFB}M_s)$; the in-plane saturation field is thus $H_{sat} = -2J_1/(t_{CFB}M_s)$. Using the $M_s$ value ($M_s = 1200\,\text{emu/cm}^3$, measured by VSM) and the saturation fields deduced from hysteresis loops shown in Fig. 1, the corresponding coupling constants are $J_1 = -0.45$, $-0.2$, $-0.14$, and $-0.0013\,\text{ergs/cm}^2$, respectively for $t_{Ru} = 0.5, 0.6, 0.8$, and 1 nm. Note the very weak value of the antiferromagnetic interaction for the 1-nm-thick Ru spacer.

Typical BLS spectra are displayed in Fig. 2 for two Ru thicknesses at $k_{SW} = 20.45$ and $8.08\,\text{rad}/\mu\text{m}$ and for two in-plane applied fields sufficient to saturate the magnetizations. Two main features are noticeable: One line (acoustic) is observable in the S and AS parts of each spectrum; the positions of these lines are not symmetrical. As the structure is made of two coupled FM layers, one expects two magnetic modes (optic and acoustic modes) in the Stokes and anti-Stokes

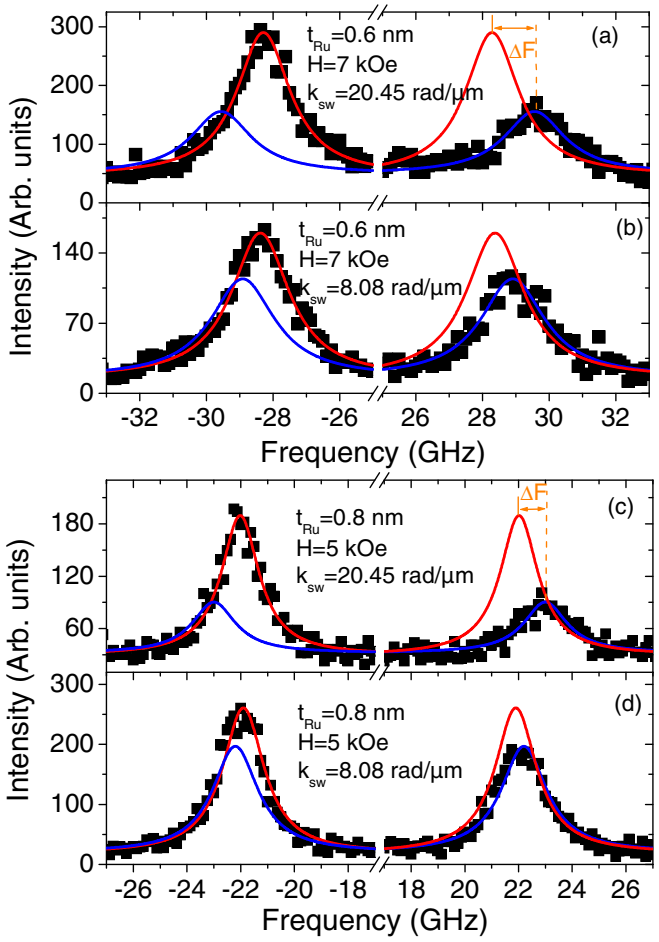


FIG. 2. BLS spectra measured for Pt/CoFeB(1.12 nm)/Ru($t_{Ru}$)/CoFeB(1.12 nm)/MgO with two Ru thicknesses ($t_{Ru}$) at 7 kOe [(a) and (b)] and 5 kOe [(c) and (d)] in-plane applied magnetic field values and at two characteristic light incidence angles corresponding to $k_{SW} = 8.08$ and $20.45\,\text{rad}/\mu\text{m}$. Symbols refer to the experimental data and solid lines are the Lorentzian fits. Fits corresponding to negative applied fields are presented for clarity and a direct comparison of the Stokes and anti-Stokes frequencies.

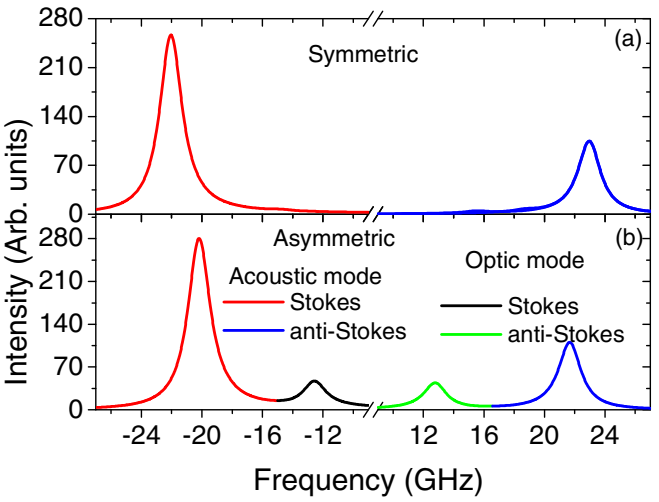


FIG. 3. Example of BLS spectra for Pt/CoFeB(1.12 nm)/Ru(0.8 nm)/CoFeB(1.12 nm)/MgO submitted to 5 kOe applied magnetic field. These simulations are obtained using our model presented in Ref. [23], including iDMI boundary conditions of Ref. [9], $M_s = 1200\,\text{emu/cm}^3$, $J_1 = -0.14\,\text{ergs/cm}^2$, gyromagnetic factor of 30.13 GHz/T, $k_{SW} = 20.45\,\text{rad}/\mu\text{m}$, $D_{eff} = -0.84\,\text{mJ/m}^2$, and (a) perpendicular anisotropy field $H_\perp = 9.3$ and 9.7 kOe for the bottom and top CoFeB layers, respectively. For (b), the same parameters with $H_\perp = 9.3$ and 13.3 kOe for the bottom and top CoFeB layers, respectively, have been used. Note the existence of two clearly intense modes in (b) due to the perpendicular anisotropy field difference between the top and the bottom CoFeB layers.

parts, as mentioned above. Nevertheless, intensity calculations (similar to those in Ref. [23] and including the iDMI boundary conditions of Ref. [9]) using the magnetic parameters deduced from the field dependence of the frequency modes (not shown here), the gyromagnetic factor of 30.13 GHz/T, measured by ferromagnetic resonance, and the iDMI effective constant $D_{eff} = -0.84\,\text{mJ/m}^2$ (deduced from BLS measurements of Pt/CoFeB/Ru, which will be presented below), reveal that the intensity of the second line (optic mode) is very weak and thus experimentally unobservable. Indeed, in the case of similarly coupled ferromagnetic films, the optic mode profile presents opposite signs in the ferromagnetic layers, thus leading to a vanishing resultant. This is because the CoFeB layers have the same thickness and not very different perpendicular anisotropy fields (400 Oe), as shown in Fig. 3(a) for $t_{Ru} = 0.8$ nm. To observe this optic mode, the perpendicular anisotropy difference should be significant, as shown in Fig. 3(b), where spectra calculations are presented for $t_{Ru} = 0.8$ nm but assuming an anisotropy field difference of 4 kOe.

The observed frequency difference between S and AS lines ($\Delta F = F_S - F_{AS}$, where $F_S$ and $F_{AS}$ are the frequencies of S and AS lines, respectively) of the acoustic mode should be related *inter alia* to iDMI. Nevertheless, simulations (close to the ones presented in Ref. [24] and complemented with iDMI boundary conditions of Ref. [9]) shown in Fig. 4(a) reveal that the frequency shift for symmetrical CoFeB layers with similar magnetic properties should be independent of the IEC strength and thus of the Ru thickness. It is noticeable that $\Delta F$ for the optic mode (not observed) is slightly IEC dependent but its variation would not be experimentally detected, according

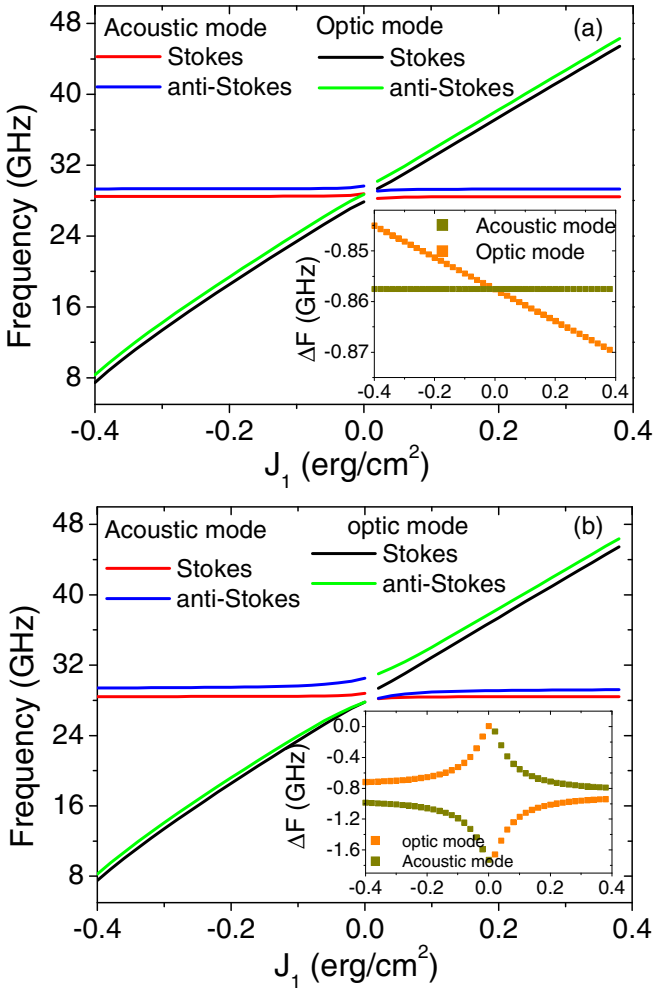


FIG. 4. Simulations showing the variation of the frequencies of the two excited modes (acoustic and optic modes) in Pt/CoFeB(1.12 nm)/Ru/CoFeB(1.12 nm)/MgO vs the bilinear interlayer exchange coupling constant $J_1$ for in-plane magnetic applied 7 kOe, $k_{sw} = 20.45\,\mathrm{rad}/\mu\mathrm{m}$, and (a) $H_\perp = 9.4$ and 9.4 kOe for the bottom and top CoFeB layers, respectively. For (b), $H_\perp = 8.6$ and 10.2 kOe for the bottom and top CoFeB layers, respectively. Simulations are based on the model in Ref. [24] complemented with iDMI boundary conditions of Ref. [9], using the other parameters of Fig. 3. The insets of (a) and (b) are the frequency differences corresponding to acoustic and optic modes.

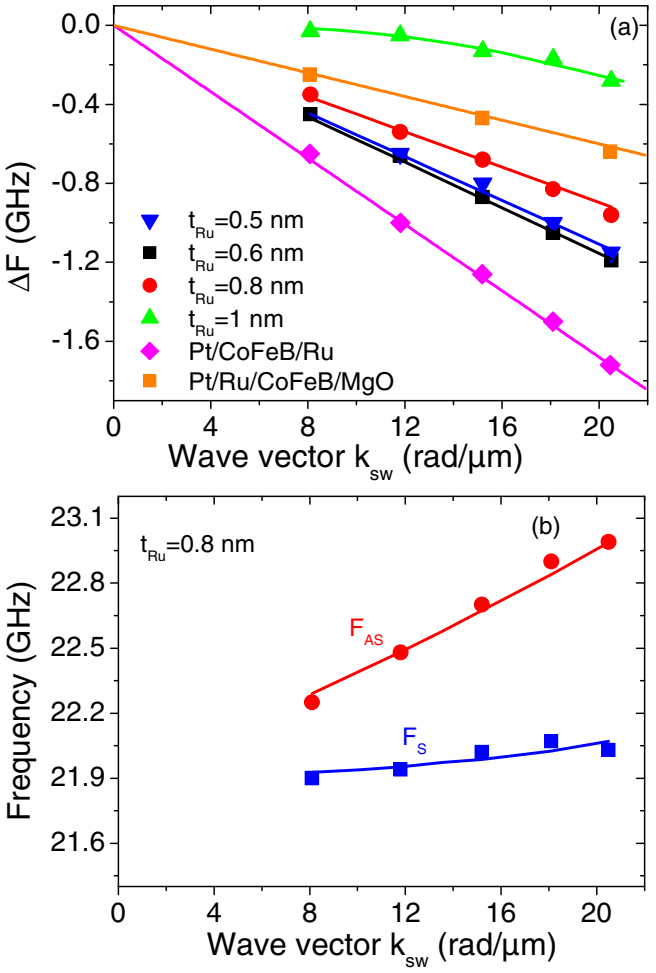


FIG. 5. (a) Wave-vector ($k_{SW}$) dependence of the experimental frequency difference $\Delta F$ of Pt/CoFeB(1.12 nm)/Ru($t_{Ru}$)/CoFeB(1.12 nm)/MgO of various Ru thicknesses $t_{Ru}$ as well as those of the Pt/CoFeB(1.12 nm)/Ru(0.8 nm) and Pt/Ru(0.8 nm)/CoFeB(1.12 nm)/MgO. (b) $k_{SW}$ dependence of the experimental frequency of the observed mode (acoustic mode) of Pt/CoFeB(1.12 nm)/Ru(0.8 nm)/CoFeB(1.12 nm)/MgO for 5 kOe in-plane magnetic field. Solid lines refer to fits using the model described in the paper, the anisotropy field differences shown in Fig. 6(a), and $D_{eff} = -0.84\,\mathrm{mJ/m^2}$ for Pt/CoFeB(1.12 nm)/Ru($t_{Ru}$)/CoFeB(1.12 nm)/MgO and for Pt/CoFeB(1.12 nm)/Ru(0.8 nm) and $D_{eff} = -0.3\,\mathrm{mJ/m^2}$ for Pt/Ru(0.8 nm)/CoFeB(1.12 nm)/MgO.

to the inset in Fig. 4(a). Moreover, the $\Delta F$ value for the acoustic mode is half of that for a single layer (according to Ref. [13], $\Delta F = \frac{2\gamma}{\pi M_s} D_{\mathrm{eff}} k_{\mathrm{SW}} = 1.72$ GHz), and it turns out that the coupled layers behave as a single layer with a double thickness. For systems having the same FM layer thicknesses and different perpendicular anisotropies, $\Delta F$ is IEC dependent [Fig. 4(b)]. For antiferromagnetic coupled layers [considered in Fig. 4(b)], the SW nonreciprocity of the acoustic mode presents a maximum in the vicinity of $J_1 = 0$.

The experimental $k_{SW}$ dependences of $\Delta F$ for various Ru thicknesses as well as those of the Ta(3 nm)/Pt(3 nm)/CoFeB(1.12 nm)/Ru(0.8 nm)/Ta(3 nm) and Ta(3 nm)/Pt(3 nm)/Ru(0.8 nm)/CoFeB(1.12 nm)/MgO(1 nm)/Ta(3 nm) individual layers are shown in Fig. 5(a). Note the negative sign of $\Delta F$, the variation of its slope with the Ru thickness, and its small value compared to that of the single CoFeB layer [Ta(3 nm)/Pt(3 nm)/CoFeB(1.8 nm)/Ru(0.8 nm)/Ta(3 nm)]. The effective iDMI constants ($D_{\mathrm{eff}}$) of the individual layers, deduced from the slope of $k_{SW}$ dependences of $\Delta F$ [13] using the above-mentioned magnetization at saturation and the gyromagnetic ratio values, are found to be $-0.84$ and $-0.3\,\mathrm{mJ/m^2}$, respectively, for Pt/CoFeB(1.12 nm)/Ru (0.8 nm) and Pt/Ru(0.8 nm)/CoFeB(1.12 nm)/MgO. This iDMI constant of Pt/CoFeB(1.12 nm)/Ru(0.8 nm) is in good agreement with that obtained by Tacchi [25] and Di [14]. The smaller iDMI value of Pt/Ru(0.8 nm)/CoFeB(1.12 nm)/MgO suggests that the thin Ru layer partially screens the interaction between Pt and CoFeB atoms and does not completely cancel

iDMI. This is in agreement with the observations of Tacchi *et al.* [25] that indicate that not only the interface Pt atoms are involved in iDMI but at least a 1-nm-thick Pt layer is concerned. The screening effect via Ir and Au spacers between Pt and the ferromagnetic layer has been reported by Robinson *et al.* [26]. The iDMI cancellation would occur for a spacer thickness of about 1 nm. We thus strongly believe that iDMI is mainly induced by Pt in our samples. Since the substrate/seed layer/HM layer/FM layer structure has not been changed in IEC samples, the iDMI constant was assumed to be the same for all samples presenting the same sequence. Consequently, the experimentally observed IEC dependence of $\Delta F$ is an indication that the bottom and top CoFeB layers have a different perpendicular anisotropy, as shown by simulations [Fig. 4(b)]. Therefore, the experimental data have been fitted using the same iDMI parameter $D_{\text{eff}} = -0.84\,\text{mJ/m}^2$ (of the single CoFeB layer, Pt/CoFeB/Ru), the above-mentioned values of $J_1$, and different anisotropy fields for the bottom and top CoFeB layers. For this, the experimental $k_{\text{SW}}$ dependence of the S and AS frequencies of each sample are fitted, as illustrated, for example, in Fig. 5(b) for $t_{\text{Ru}} = 0.8\,\text{nm}$, and $\Delta F$ is then calculated. The $t_{\text{Ru}}$ dependence of these anisotropy fields is shown in Fig. 6(a), where higher anisotropy fields have been observed for the top CoFeB with thinner Ru layers. As the Ru thickness increases, the anisotropy difference decreases and changes sign for a Ru thickness of around 1 nm. Indeed, while the bottom FM layer anisotropy would keep increasing with the spacer thickness, the top FM layer anisotropy would slightly vary. Regardless of the spacer thickness, the top FM layer is always deposited on a Ru layer, yielding a constant effect on the FM layer. At variance, the thicker the spacer is, the higher its effect on the bottom layer is. This feature could be interpreted, for instance, by assuming the top FM layer atomic structure would be imposed by the Ru layer, while the bottom FM layer would have a different atomic structure whose parameter would vary with the spacer thickness because of strain induced by the Ru layer. This Ru thickness dependence is in agreement with the observed behavior of the perpendicular anisotropy in Ru/Co/Ru systems, presented by Kolesnikov *et al.* [27], who showed that it is very sensitive to the Ru layer thickness. Therefore, since the Ru spacer thickness varies from one sample to another, it is expected that the interface anisotropy changes with Ru thickness, as shown in Fig. 6(a). This anisotropy field difference is thus due to the perpendicular interface anisotropy induced by the different buffer and capping layers used here (Pt, Ru, and MgO). Moreover, this interface anisotropy has been confirmed experimentally by investigating the thickness dependence of effective magnetization ($4\pi M_{\text{eff}} = 4\pi M_s - H_\perp$) of the individual ferromagnetic layers Ta(3 nm)/Pt(3 nm)/Ru(0.8 nm)/CoFeB($t_{\text{CFB}}$)/MgO(1 nm)/Ta(3 nm) and Ta(3 nm)/Pt(3 nm)/CoFeB($t_{\text{CFB}}$)/Ru(0.8 nm)/Ta(3 nm) of variable CoFeB thicknesses, shown in Fig. 6(b). The $M_{\text{eff}}$ values have been deduced from the fit of the experimental field dependence of the uniform precession mode frequency measured via ferromagnetic resonance. Using the above-mentioned value of $M_s$, the interface anisotropy was found to be 1.02 and $0.68\,\text{ergs/cm}^2$ for Pt/Ru(0.8 nm)/CoFeB/MgO and Pt/CoFeB/Ru(0.8 nm), respectively.

This feature of different anisotropy fields is very important to correctly evaluate the iDMI parameter and explain the frequency mismatch. In order to understand how this anisotropy field difference affects the spin-wave nonreciprocity, the profile of the perpendicular to the plane component of the magnetization versus the stack thickness for Pt/CoFeB(1.12 nm)/Ru(0.8 nm)/CoFeB(1.12 nm)/MgO has been simulated. Figure 7 shows the obtained profile over the stack depth for two different bilinear IEC constants ($J_1 = 0$ and $J_1 = -0.14\,\text{ergs/cm}^2$) and for CoFeB films having similar ($H_\perp = 9.5\,\text{kOe}$ for both CoFeB layers) or different anisotropy fields ($H_\perp = 7.5$ and 11.5 kOe for the bottom and top CoFeB layers, respectively) subjected to iDMI ($D_{\text{eff}} = 0$ or $-0.84\,\text{mJ/m}^2$) under a 5 kOe in-plane applied magnetic field. Note that 0 corresponds to the beginning of the top CoFeB layer. The profiles have been calculated using the fluctuation dissipation theorem as the line intensity calculations presented in Fig. 3. The displayed curves correspond to the square of the magnitude of the thermoactivated dynamic magnetization

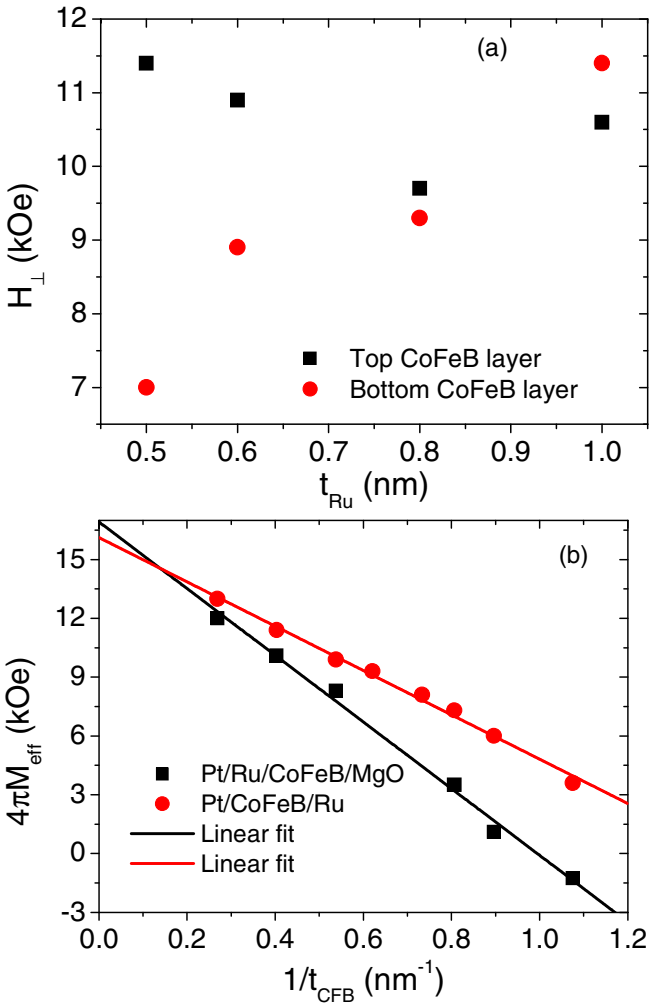


FIG. 6. (a) Ru thickness dependence of the perpendicular anisotropy field deduced from fits of the experimental data of Fig. 5(a). (b) CoFeB thickness dependence of the effective magnetization ($4\pi M_{\text{eff}}$) extracted from the fit of ferromagnetic resonance measurements of Pt/CoFeB($t_{\text{CFB}}$)/Ru(0.8 nm) and Pt/Ru(0.8 nm)/CoFeB($t_{\text{CFB}}$)/MgO. Symbols refer to experimental data while solid lines are the linear fits.

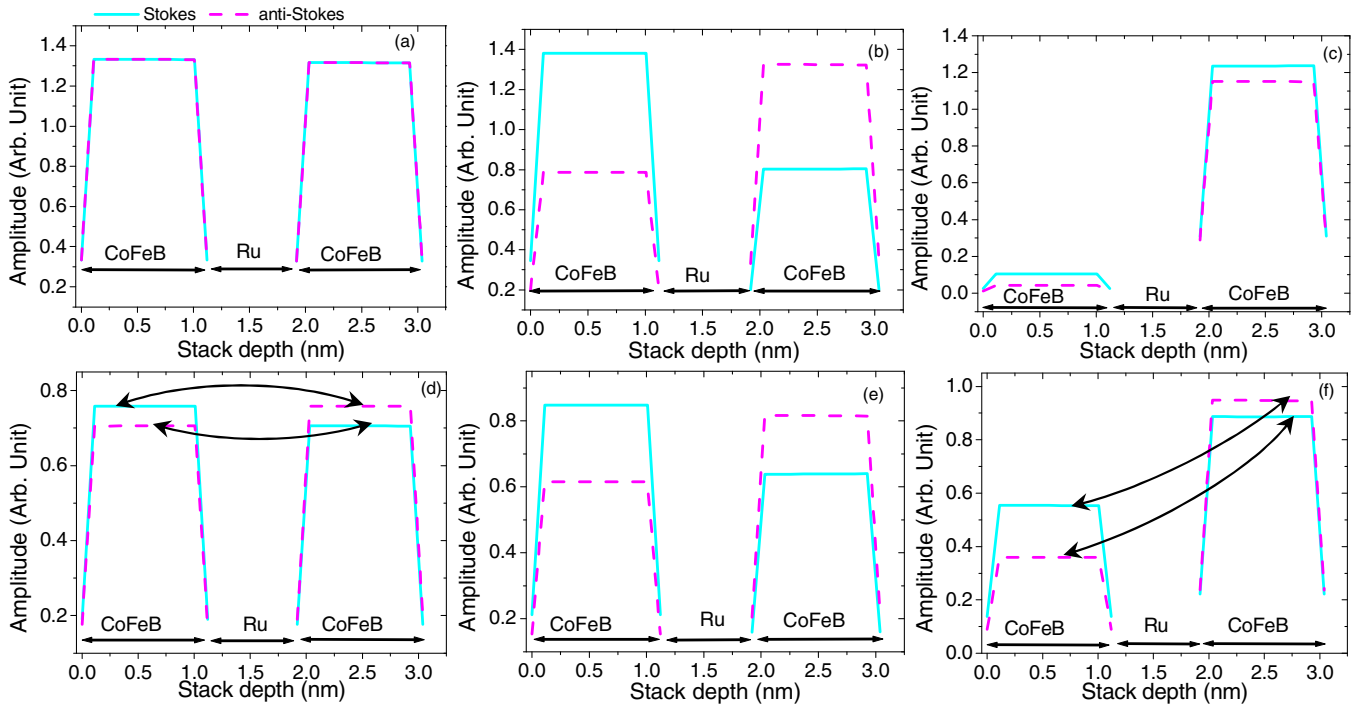


FIG. 7. Profile of the perpendicular to the plane component of the thermoactivated dynamic magnetization for Stokes (cyan solid line) and anti-Stokes (magenta dashed line) modes vs the stack depth for Pt/CoFeB(1.12 nm)/Ru(0.8 nm)/CoFeB(1.12 nm)/MgO systems submitted to 5 kOe in-plane applied magnetic field. The first and second columns correspond to calculations for CoFeB films having similar anisotropy fields ($H_\perp = 9.5$ kOe for both CoFeB layers) while the third column refers to simulations for CoFeB films with different anisotropy fields ($H_\perp = 7.5$ and 11.5 kOe for the bottom and top CoFeB layers, respectively). Different cases corresponding to (a) $J_1 = 0$ and $D_{\text{eff}} = 0$, (b) $J_1 = 0$ and $D_{\text{eff}} = -0.84\,\text{mJ/m}^2$, (c) $J_1 = 0$ and $D_{\text{eff}} = -0.84\,\text{mJ/m}^2$, (d) $J_1 = -0.14\,\text{ergs/cm}^2$ and $D_{\text{eff}} = 0$, (e) $J_1 = -0.14\,\text{ergs/cm}^2$ and $D_{\text{eff}} = -0.84\,\text{mJ/m}^2$, and (f) $J_1 = -0.14\,\text{ergs/cm}^2$ and $D_{\text{eff}} = -0.84\,\text{mJ/m}^2$ are considered. Note that for the stack depth, 0 corresponds to the beginning of the top CoFeB layer. Arrows indicate profiles which should be compared to understand the frequency mismatch.

component perpendicular to the films. In order to understand the influence of both iDMI and anisotropy asymmetry on the frequency mismatch, the profile of the Stokes mode will be compared to the anti-Stokes one. If these profiles are the same when mirrored with respect to the median plane of the CoFeB/Ru/CoFeB stack, then the corresponding frequencies are equal. Different mirrored profiles imply a frequency mismatch. Therefore, the profile asymmetry extent measures the frequency difference. Indeed, in the perfectly symmetric case with $D_{\text{eff}} = 0$ and $H_\perp = 9.5$ kOe for both CoFeB layers, regardless of the exchange coupling value, the calculated profile of the AS mode is obtained by symmetry with respect to the median plane from the calculated profile for the S mode [Figs. 7(a) and 7(d) for $J_1 = 0$ and $-0.14\,\text{ergs/cm}^2$, respectively]. Consequently, $F_S$ and $F_{AS}$ are equal. In the presence of iDMI ($D_{\text{eff}} = -0.84\,\text{mJ/m}^2$), the S and AS profiles are no longer symmetric with respect to the median plane, but this asymmetry [Fig. 7(b) for $J_1 = 0$] does not depend on the exchange coupling $J_1$ [Fig. 7(c) for $J_1 = -0.14\,\text{ergs/cm}^2$]. Therefore, $F_S$ and $F_{AS}$ are different but the frequency difference does not vary with the $J_1$ value, as already mentioned in Fig. 4(a) (acoustic mode). Finally, in the case of asymmetric magnetic anisotropies ($H_\perp = 7.5$ and 11.5 kOe for the bottom and top CoFeB layers, respectively) with iDMI, the S and AS profiles are not symmetric with respect to the median plane and this asymmetry is more pronounced for $J_1 = 0$ [Fig. 7(c)] when compared to that for $J_1 = -0.14\,\text{ergs/cm}^2$ [Fig. 7(f)]. This feature can be related to the frequency difference variation with the exchange coupling, as presented in Fig. 4(b). Finally, the influence of both iDMI and anisotropy asymmetry on the frequency difference can be explained by the effect of iDMI and anisotropy asymmetry on the eigenmode profiles.

## IV. CONCLUSION

This paper presents an experimental and theoretical study of stacks made of two coupled ferromagnetic layers deposited on a heavy metal inducing an interface Dzyaloshinskii-Moryia interaction. The static measurements prove that the coupled layers have spontaneous opposite magnetizations and enable one to derive the coupling between the two ferromagnetic layers. The spin-wave observations by means of Brillouin light scattering reveal a Stokes and anti-Stokes frequency difference that could be related to the interface Dzyaloshinskii-Moryia interaction. Nevertheless, the simulations show that the frequency difference is also influenced by the coupling between the ferromagnetic layers when they possess different anisotropies. Magnetization profile calculations allowed us to explain this frequency mismatch by including the anisotropy field difference between the top and bottom ferromagnetic layers of the stack. Therefore, the interface Dzyaloshinskii-Moryia interaction parameter is correctly derived once the different anisotropies are evaluated.

**ACKNOWLEDGMENT**

This work has been supported by the Conseil regional d'Île-de-France through the DIM NanoK (BIDUL project) and by USPC-NUS via the project IMANSA No. 2016-R/USPC-NUS. M.S.G and T.P. acknowledge the financial support of UEFISCDI through PN-II-RU-TE-2014-1820 — SPINCOD research Grant No. 255/01.10.2015.

[1] W. Heisenberg, Z. Phys. **49**, 619 (1928).
[2] I. E. Dzyaloshinskii, Sov. Phys. JETP **5**, 1259 (1957).
[3] T. Moriya, Phys. Rev. **120**, 91 (1960).
[4] J. Kishine and A. Ovchinnikov, Solid State Phys. **66**, 1 (2015).
[5] U. K. Roszler, A. N. Bogdanov, and C. Pfleiderer, Nature (London) **442**, 797 (2006).
[6] C. Felser, Angew. Chem., Int. Ed. **52**, 1631 (2013).
[7] N. Nagaosa and Y. Tokura, Nat. Nanotechnol. **8**, 899 (2013).
[8] A. Thiaville, S. Rohart, E. Jué, V. Cros, and A. Fert, Europhys. Lett. **100**, 57002 (2012).
[9] M. Kostylev, J. Appl. Phys. **115**, 233902 (2014).
[10] S. Pizzini, J. Vogel, S. Rohart, L. D. Buda-Prejbeanu, E. Jué, O. Boulle, I. M. Miron, C. K. Safeer, S. Auffret, G. Gaudin, and A. Thiaville, Phys. Rev. Lett. **113**, 047203 (2014).
[11] S. Emori, E. Martinez, K.-J. Lee, H.-W. Lee, U. Bauer, S.-M. Ahn, P. Agrawal, D. C. Bono, and G. S. D. Beach, Phys. Rev. B **90**, 184427 (2014).
[12] J. Torrejon, J. Kim, J. Sinha, S. Mitani, M. Hayashi, M. Yamanouchi, and H. Ohno, Nat. Commun. **5**, 4655 (2014).
[13] M. Belmeguenai, J.-P. Adam, Y. Roussigné, S. Eimer, T. Devolder, J.-V. Kim, S. M. Chérif, A. Stashkevich, and A. Thiaville, Phys. Rev. B **91**, 180405(R) (2015).
[14] K. Di, V. L. Zhang, H. S. Lim, S. C. Ng, M. H. Kuok, X. Qiu, and H. Yang, Appl. Phys. Lett. **106**, 052403 (2015).
[15] S. S. P. Parkin and D. Mauri, Phys. Rev. B **44**, 7131 (1991).
[16] S. S. P. Parkin, Phys. Rev. Lett. **67**, 3598 (1991).
[17] P. Grünberg, R. Schreiber, Y. Pang, M. B. Brodsky, and H. Sower, Phys. Rev. Lett. **57**, 2442 (1986).
[18] B. N. Engel, J. Åkerman, B. Butcher, R. W. Dave, M. DeHerrera, M. Durlam, G. Grynkewich, J. Janesky, S. V. Pietambaram, N. D. Rizzo, J. M. Slaughter, K. Smith, J. J. Sun, and S. Tehrani, IEEE Trans. Magn. **41**, 132 (2005).
[19] M. Belmeguenai, T. Martin, G. Woltersdorf, M. Maier, and G. Bayreuther, Phys. Rev. B **76**, 104414 (2007).
[20] G. Chen, A. Mascaraque, A. T. N'Diaye, and A. K. Schmid, Appl. Phys. Lett. **106**, 242404 (2015).
[21] S. D. Pollard, J. A. Garlow, J. Yu, Z. Wang, Y. Zhu, and H. Yang, Nat. Commun. **8**, 14761 (2017).
[22] V. L. Zhang, K. Di, H. S. Lim, S. C. Ng, M. H. Kuok, J. Yu, J. Yoon, X. Qiu, and H. Yang, Appl. Phys. Lett. **107**, 022402 (2015).
[23] Y. Roussigné, F. Ganot, C. Dugautier, P. Moch, and D. Renard, Phys. Rev. B **52**, 350 (1995).
[24] B. Hillebrands, Phys. Rev. B **41**, 530 (1990).
[25] S. Tacchi, R. E. Troncoso, M. Ahlberg, G. Gubbiotti, M. Madami, J. Åkerman, and P. Landeros, Phys. Rev. Lett. **118**, 147201 (2017).
[26] R. M. Rowan-Robinson, A. A. Stashkevich, Y. Roussigne, M. Belmeguenai, S.-M. Cherif, A. Thiaville, T. P. A. Hase, A. T. Hindmarch, and D. Atkinson, arXiv:1704.01338 [Sci. Rep. (to be published)].
[27] A. G. Kolesnikov, M. E. Stebliy, A. V. Ognev, A. S. Samardak, A. N. Fedorets, V. S. Plotnikov, X. Han, and L. A. Chebotkevich, J. Phys. D: Appl. Phys. **49**, 425302 (2016).